

PAPER DETAILS

TITLE: A GRAPHENE-BASED MONOPOLE MICROSTRIP ANTENNA WITH TUNEABLE BANDGAP FOR UWB IMPLEMENTATIONS

AUTHORS: Mustafa Alasadi,Oguz Karan


PAGES: 277-290

ORIGINAL PDF URL: <https://dergipark.org.tr/tr/download/article-file/3383544>


A GRAPHENE-BASED MONOPOLE MICROSTRIP ANTENNA WITH TUNEABLE BANDGAP FOR UWB IMPLEMENTATIONS

Mustafa Kareem Najim AL-ASADI^{*1}, Oğuz KARAN²

¹ Department of Electrical and Computer Engineering, Altınbaş University, İstanbul, Türkiye
mustafakareem909@gmail.com

( <https://orcid.org/0009-0003-3840-0333>)

² Department of Electrical and Computer Engineering, Altınbaş University, İstanbul, Türkiye
oguz.karan@altinbas.edu.tr

( <https://orcid.org/0000-0003-2962-4653>)

Received: 04.09.2023

Accepted: 15.11.2023

Published: 31.12.2023

*Corresponding author

Research Article

pp.277-290

DOI: 10.53600/ajesa.1354785

Abstract

Monopole Microstrip Antennas (M-MSAs) are widely used because of their price, ease of manufacturing, and compact size, making them ideal for portable applications. Nowadays, Ultrawide Band (UWB) technology, used in wireless applications, relies on this antenna. The UWB frequency range is 3.1 to 10.6 GHz, allowing low-power wireless applications such as wireless music, personal localization, radio frequency recognition, radar, and HD video dissemination. However, this frequency band's broadness increases interference. This contribution research formulates simulates, and optimises a modified small-square M-MSA that meets UWB technology's huge bandwidth requirements. A square radiated patch, a dielectric material with a thickness of 1 mm and 4.7 relative permittivity, a partly ground plane printed on the patch's face, and a coplanar waveguide feed make up the M-MSA design. The M-MSA design is modified to reduce the patch's bottom corners and change its proportions to enable compatibility with the UWB complete band. A U-shaped aperture on the patch should be etched to produce a bandgap in UWB frequencies, reducing interference. Filling the aperture with graphene allows bandgap tunability. The graphene's bandgap dissipates with DC voltage, but without biasing, its high impedance restricts aperture current flow. The bandgap's effect is seen at 3.87-4.85 GHz. After simulation and tweaking, gain and efficiency improved significantly. The bandgap region, which was chosen to reduce interference from military fixed communications, mobile communications, unmanned aerial vehicles, short-range radio links, satellite communications, and the low band of 5G, also exhibits a significant increase in attenuation and gain degradation.

Keywords: 5G, M-MSA, Coplanar waveguide, graphene, UWB.

UWB UYGULAMALARI İÇİN AYARLANABİLİR BANT ARALIĞINA SAHİP GRAFEN TABANLI TEK KUTUPLU MİKROŞERİT ANTEN

Özet

Monopol Mikroşerit Antenler (M-MSA'lar), fiyatları, üretim kolaylıkları ve kompakt boyutları nedeniyle yaygın olarak kullanılmaktadır ve bu da onları taşınabilir uygulamalar için ideal kılmaktadır. Günümüzde kablosuz uygulamalarda kullanılan Ultrawide Band (UWB) teknolojisi bu antene dayanmaktadır. UWB frekans aralığı 3,1 ila 10,6 GHz olup, kablosuz müzik, kişisel konum belirleme, radyo frekansı tanıma, radar ve HD video dağıtımı gibi düşük güçlü kablosuz uygulamalara olanak tanır. Ancak bu frekans bandının genişliği girişimi artırmaktadır. Bu katkı araştırması, UWB teknolojisinin büyük bant genişliği gereksinimlerini karşılayan değiştirilmiş küçük kare M-MSA'nın simüle edilmesini ve optimize edilmesini formüle eder. Kare yayılan bir yama, 1 mm kalınlığında ve 4,7 bağlı geçirgenliğe sahip bir dielektrik malzeme, yamanın yüzüne basılmış kısmen yer düzlemi ve eş düzlemli bir dalga kılavuzu beslemesi M-MSA tasarımını oluşturur. M-MSA tasarımı, yamanın alt köşelerini azaltacak ve UWB tam bandıyla uyumluluğu sağlamak için oranlarını değiştirecek şekilde değiştirildi. UWB frekanslarında paraziti azaltacak bir bant aralığı oluşturmak için yama üzerinde U şeklinde bir açıklık kazınmalıdır. Açıklığın grafenle doldurulması bant aralığının ayarlanmasına olanak tanır. Grafenin bant aralığı DC voltajıyla birlikte dağılır, ancak öngerilim olmadan yüksek empedansı açıklık akım akışını kısıtlar. Bant aralığının etkisi 3,87-4,85 GHz'de görülüyor. Simülasyon ve ince ayardan sonra kazanç ve verimlilik önemli ölçüde arttı. Askeri sabit iletişim, mobil iletişim, insansız hava araçları, kısa menzilli radyo bağlantıları, uydu iletişimleri ve 5G'nin düşük bandından kaynaklanan paraziti azaltmak için seçilen bant aralığı bölgesi, aynı zamanda zayıflama ve kazanım bozulmalarında da önemli bir artış sergiliyor

Anahtar Kelimeler: 5G, M-MSA, Eş düzlemli dalga kılavuzu, grafen, UWB.

1. Introduction

Wireless communications through Ultra-Wideband (UWB) technology have witnessed remarkable advancements in recent years. UWB is a wireless communication technology that utilizes a wide spectrum of frequencies, typically spanning several gigahertz, to enable high-speed data transmission with low power consumption. This unique characteristic of UWB opens up a wide range of applications across various industries, including healthcare, automotive, industrial automation, and consumer electronics (Ahmad et al.2022).

In the healthcare sector, UWB-based communication systems have been instrumental in the development of real-time, high-precision location tracking for medical equipment and personnel within healthcare facilities. This has significantly improved patient care, as it allows for the rapid response to emergencies and ensures the efficient management of medical resources. In the automotive industry, UWB technology plays a pivotal role in enhancing vehicle safety through the implementation of advanced driver assistance systems (ADAS). UWB sensors enable precise vehicle localization, which is crucial for features like adaptive cruise control, lane-keeping assistance, and collision avoidance systems. These capabilities are integral to the evolution of autonomous driving technology (Zhao et al. 2023; Bastida Castillo et al.2018).

Moreover, UWB's ability to provide secure and accurate indoor positioning has found applications in industrial automation. This technology facilitates the tracking of assets and enhances the efficiency of manufacturing processes. It ensures seamless coordination between robots and machinery, contributing to increased productivity and reduced downtime in factories. In consumer electronics, UWB has enabled the development of seamless, secure, and high-speed file-sharing methods between devices. This has revolutionized the way we interact with technology, making it easier to transfer large files, connect smart devices, and improve the overall user experience. Despite its promising applications, UWB technology also faces its share of challenges. Ensuring coexistence with other wireless technologies, managing interference, and addressing regulatory concerns are some of the key hurdles that researchers and engineers are actively working to overcome (Chen et al 2020; Martalo et al 2021; Ghosh & Sahu, 2016).

Microstrip antennas have become an indispensable component in UWB communication systems, seamlessly aligning with the technology's requirements and capabilities. These compact and versatile antennas offer several advantages for UWB applications. Their low profile, lightweight design, and ease of integration make them a preferred choice for UWB devices, ensuring compatibility with the diverse range of applications mentioned earlier (Perdana, Hariyadi & Wahyu, 2017).

In healthcare, microstrip antennas embedded within medical devices and wearables allow for real-time patient monitoring and data transmission with precision. Their small form factor is particularly advantageous in these applications, where space constraints and patient comfort are critical factors. In the automotive industry, UWB-enabled microstrip antennas are integrated into vehicle communication systems, providing reliable and high-speed data exchange for advanced safety features. Their compact size and ability to be seamlessly incorporated into the vehicle's design make them an ideal choice for facilitating communication between vehicles and infrastructure, enhancing road safety and traffic management. In industrial automation, microstrip antennas are deployed in UWB-based asset tracking systems, enabling precise and efficient inventory management within factories and warehouses.

Their compact nature ensures they can be easily mounted on assets or equipment, aiding in real-time monitoring and logistics optimization. Furthermore, in consumer electronics, microstrip antennas play a vital role in UWB-enabled devices, facilitating rapid data transfer between smartphones, laptops, and other gadgets. Their unobtrusive design ensures that these antennas can be integrated into the sleek and compact form factors demanded by modern consumers (Raval, Pimpalgaonkar, Chaurasia & Upadhyaya, 2016; Mahmood et al.,2020).

As UWB technology continues to advance and find applications across various sectors, microstrip antennas are expected to remain at the forefront, offering an essential solution for enabling high-speed, reliable, and precise wireless communication. Together, UWB and microstrip antennas are contributing to the realization of a connected, efficient, and safer future across industries (Tiwari & Malik, 2020).

In this paper, a small-sized monopole microstrip antenna (M-MSA) is suggested for the applications of the UWB. The simulated M-MSA comprise of a U-shaped slot etched on the patch and filled with graphene material to create a tunable bandgap that contributes to minimizing the interference from the neighboring frequencies of the other applications.

2. Antenna Simulation

In this specific section of the section, we shall thoroughly examine, elucidate, and converse about the preliminary measures required for the proposed antenna's creation. We will commence by formulating the primary design for the typical M-MSA, followed by the introduction of a U-shaped aperture carving procedure to establish the band-rejection characteristic, and ultimately integrating the graphene component to render it compatible with the engraved aperture. The layout of the proposed antenna's design is structured as a conventional M-MSA from a rectangular shape. Nevertheless, certain alterations have been made to the patch and a partial defected ground plane dimension. In order to initiate the antenna design process correctly, it is crucial to select a set of key parameters that are exclusive to the antenna. These parameters encompass the frequency of operation, the input impedance, and the characteristics of the dielectric material employed for the antenna substrate. It is imperative to recognize and determine these parameters at the outset of the design process to ensure the proper functionality of the antenna, as presented in the Table 1.

Table 1. Functional parameter for MSA design.

| Parameters | Definition |
|--------------------------|--------------------|
| Centre Frequency | 6 GHz |
| Input Impedance | 50 Ω |
| Substrate Specifications | $\epsilon_r = 4.7$ |
| | $h = 1 \text{ mm}$ |
| Conductive Material Type | Copper |

After that we trying to calculate the proposed antenna dimensions by utilising the equation of the basic transmission line method that was described in the references (Werfelli et al,2016; Hossain, Ahmed & Kabir, 2022) with the help of MATLAB software. In this design of UWB-based MSA it is necessary to meet the UWB technology requirements (i.e., frequency range and omni-directional pattern). In order to develop MSA with the mentioned criteria the ground plane must designed to be in the from a partial one or utilising the Coplanar Waveguide (CPW) feeding. In this way the ground plane is situated over the surface of the antenna (i.e., the ground plane and the patch will be engraved over the same face of the substrate). Table 2 presents the dimensions for the primary M-MSA design and Figure 1 illustrates the primary M-MSA within the environment of the simulation software.

Table 2. Calculated M-MSA dimensions.

| Parameter | Interpretation |
|---------------------------------------|----------------|
| Width for patch (W_p) | 17.76 (mm) |
| Length for patch (L_p) | 13.58 (mm) |
| Width for substrate (W_s) | 35.52 (mm) |
| Length for substrate (L_s) | 27.16 (mm) |
| Width for ground plane (W_G) | 12.38 (mm) |
| Length for ground plane (L_G) | 16.76 (mm) |
| Width for strip line (W_{STRIP}) | 2.2 (mm) |
| Length for strip line (L_{STRIP}) | 17.74 (mm) |
| Ground-Patch spacing (d) | 0.001(mm) |

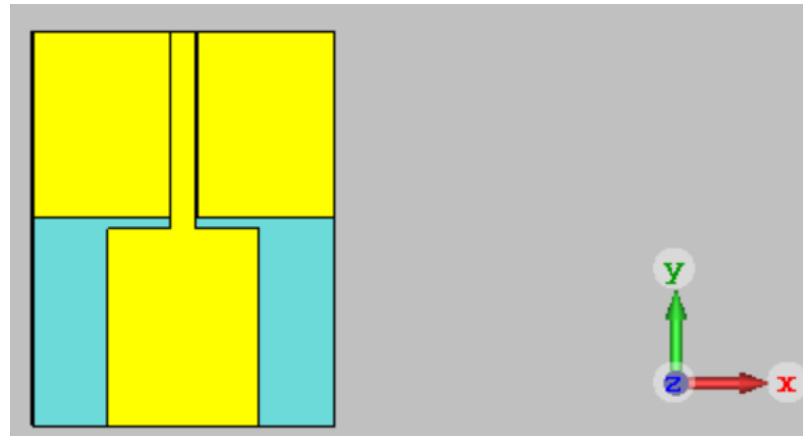


Figure 1. Simulated M-MSA

Due to the limited BW of the M-MSA, the primary design doesn't cover the whole band of the UWB the corrections on the shapes should be made. The first step is summarised by cutting the lower corners and changing the total dimensions, as exhibited in Figure 2. For such modifications, there aren't specific rules or mathematical modelling but here we are dependent on trial and error till obtaining the optimum results. Table 3 demonstrates the new dimensions for the M-MSA after parameters and shape modifications.

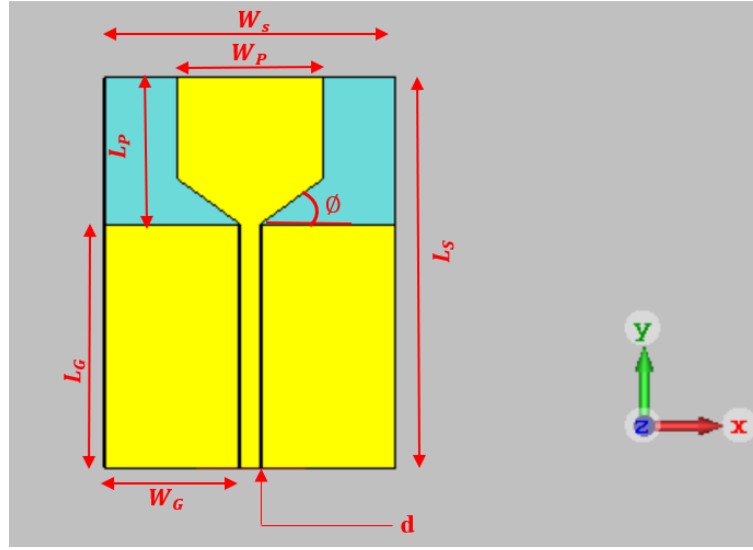


Figure 2. Simulated M-MSA after modification process.

After applied the required modifications on the dimensions and the shape we met with the characteristic of the UWB technology.

Table 3. Modified M-MSA dimensions.

| Parameter | Interpretation |
|---------------------------------------|----------------|
| Width for patch (W_p) | 16.14 (mm) |
| Length for patch (L_p) | 16.14 (mm) |
| Width for substrate (W_s) | 31 (mm) |
| Length for substrate (L_s) | 40.71 (mm) |
| Width for ground plane (W_G) | 14.15 (mm) |
| Length for ground plane (L_G) | 24.5 (mm) |
| Width for strip line (W_{STRIP}) | 2.69 (mm) |
| Length for strip line (L_{STRIP}) | 24.5 (mm) |
| Ground-Patch spacing (d) | 0.23 (mm) |

3. M-MSA With Notch-Band Characteritics

A notch-band refers to a frequency range in which the antenna exhibits significantly reduced or suppressed performance. This frequency range, often referred to as a "notch," is deliberately designed to attenuate or reject signals within a specific range. The purpose of incorporating a notch-band in a UWB antenna is to mitigate interference from specific frequencies or unwanted signals. It allows the antenna to maintain its wide bandwidth characteristics while selectively attenuating signals within the notch frequency range. This can be useful in scenarios where certain frequency bands need to be avoided or rejected, such as licensed bands or sources of interference. Various techniques, such as adding reactive components, resonant structures, or introducing filtering elements, can be used to achieve a notch-band in a UWB antenna. These design elements are meticulously engineered to produce a narrowband response within a wideband antenna structure. In this work, we suggest utilizing the U-shaped aperture to generate a certain bandgap. The selection of the U-aperture position is made based on the current distribution and

with the help of a trial-and-error approach till reaches to the notch at the required frequency band. Figure 3 illustrates the current on the patch of the M-MSA.

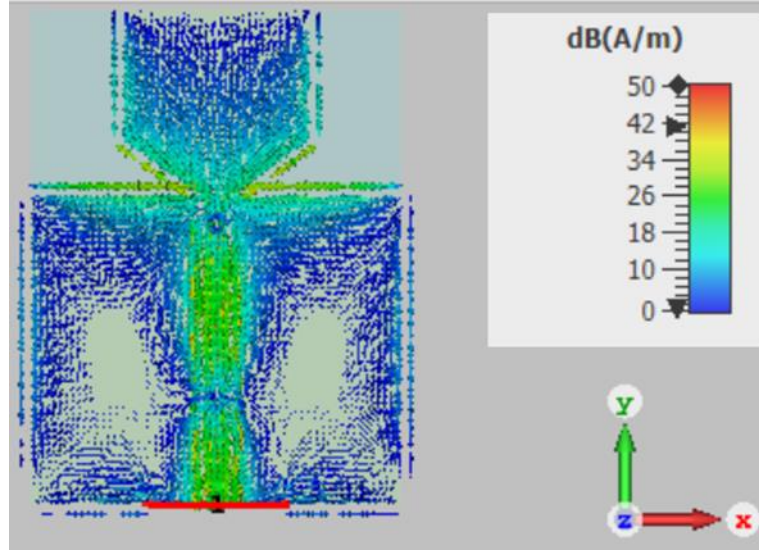
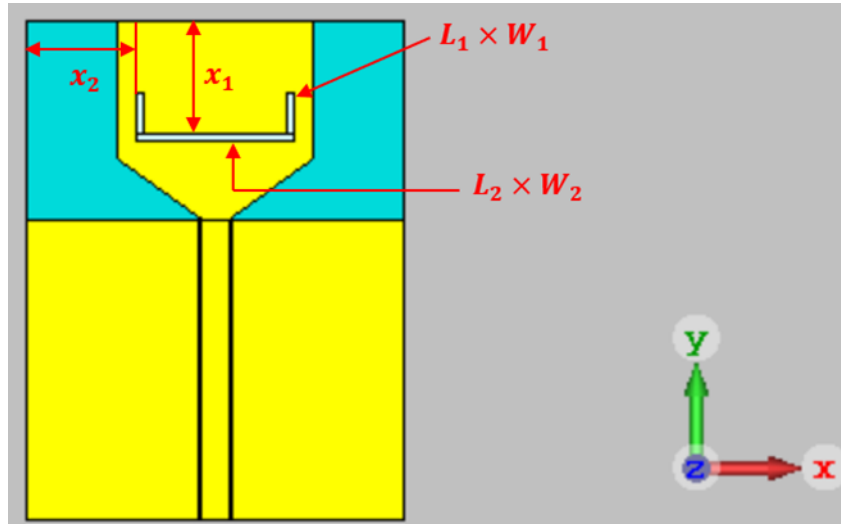


Figure 3. Current distribution on M-MSA patch.

As demonstrated in previous Figure 3, the allocation of the maximum current is presence in the strip feed line and the border of the ground plane. So, we select the position of the U-shape aperture in the location of small current at the middle of the M-MSA patch, as exhibited in Figure 4.



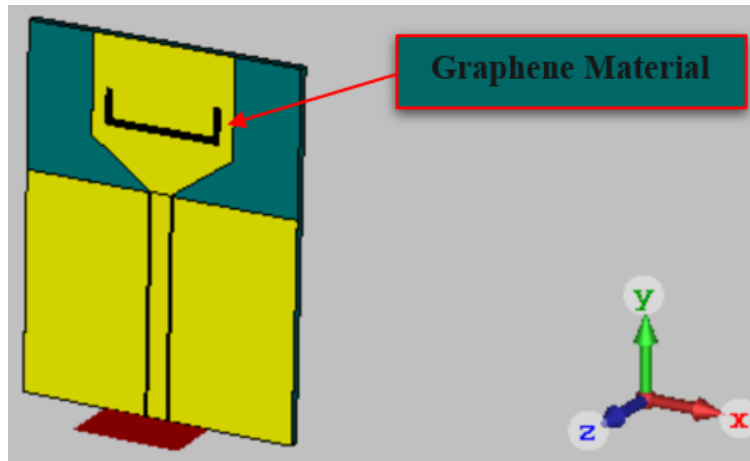
The completed size description and the location for the engraved U-shape aperture on the surface of the radiated patch of the antenna is presented in Table 4.

Table 4. Dimensions for the designed U-aperture.

| Parameter | Interpretation |
|--|----------------|
| Right arm length (L_1) | 3.21 (mm) |
| Right arm width (W_1) | 0.65 (mm) |
| Horizontal aperture length (L_2) | 0.65 (mm) |
| Horizontal aperture width (W_2) | 12.91 (mm) |
| Distance between U-aperture and upper patch edge (x_1) | 9.04 (mm) |
| Distance between U-aperture and left patch edge (x_2) | 1.6 (mm) |

4. M-MSA With Graphene-Based Notch-Band Characteristics

In some cases, the M-MSA is needed to cover the total band of the UWB system, and in other cases reject some bands like military fixed communications, mobile communications, unmanned aerial vehicles, radio links, satellite communications, and the low band of 5G to minimize the available interference from such sources. For this purpose, we exploit the variable conductivity that possesses by the graphene material. In this study, the U-aperture is filled with flakes of graphene to function as a controllable switch that is in an on state when applied DC voltage is to the graphene layer and in an off state when no biasing is applied. In the case of the DC is subjected on the layers the surface impedance is lessening and allowing the current to pass through the U-aperture here the antenna will cover the entire band of the UWB system. While in no subjected voltage its impedance will be high and prevent the current from passing then the notch is created. Figure 5 illustrates the designed M-MSA with graphene material.

**Figure 5.** Simulated M-MSA with graphene U-aperture.

The graphene material is simulated by the means of CST software as a sheet of an ohmic impedance. The values for the ON and OFF states are calculated based on the equations of the graphene conductivity that have been presented in the references (Abdulnabi, Shurij & Sohrab, 2023; Alvarez, Cheung & Thompson, 2017) with the help of the MATLAB program. Table 5 presents the values of the ON/OFF impedance and constant values.

Table 5. Parameters for graphene material modelling.

| Parameters | Values |
|--------------------------|--------------------------|
| μ_l | 2.70 m ² /Vs |
| D | 4.0 eV |
| Graphene thickness (t) | 10.0 nm |
| Room temperature (T) | 295 Kelvin |
| V_{DC_on} | 40.0 V |
| Z_{S_on} | 4.145 +j0.360 Ω / |
| V_{DC_off} | ~0.0 V |
| Z_{S_off} | 36533+j1.51 Ω / |

5. Achieved Results

In this section, we will interpret and discuss the obtained results following the finishing of the simulation procedure by the CST workspace for all cases of designs. The results include the M-MSA return loss (S_{11}), the M-MSA BW, and the M-MSA gain.

5.1 Results for Primary Design

In this subsection, we will present the results for the primary M-MSA design before the parameters and shape modifications process.

a) M-MSA S_{11}

An important factor used to evaluate the effectiveness and impedance matching of an antenna system is antenna S_{11} . It measures the power that is reflected back toward the source due to imperfections in the antenna, transmission line, or environment. The S_{11} , which is frequently expressed in decibels (dB), is an important sign of how well an antenna transmits or receives electromagnetic signals. However, impedance mismatches do happen in real-world situations, which causes some of the signals to be reflected back. Greater inefficiency and more power are lost as a result of reflections, as indicated by higher S_{11} values. Engineers can assess and improve antenna performance for better signal transmission and reception by measuring return loss. Commonly the S_{11} should be less than or equal -10 dB which

means the M-MSA extradited a 90% of power of the source and the remainder is reflected back to the source. Figure 6 shows the acquired S_{11} results for the primary M-MSA design.

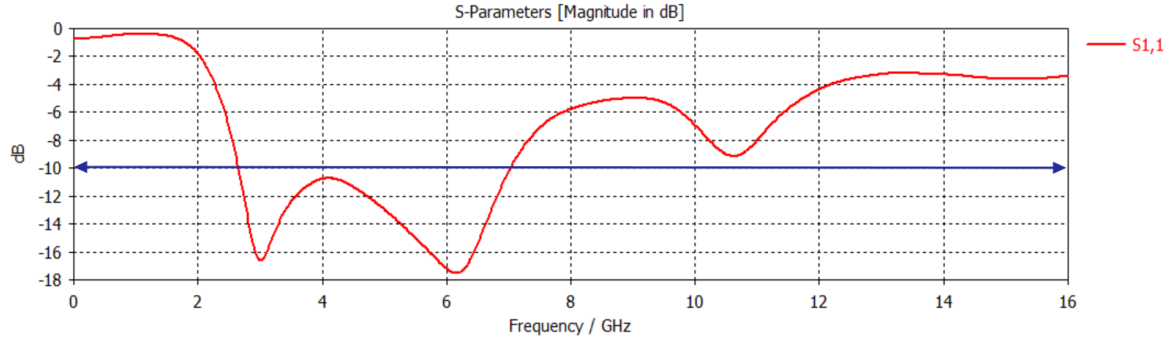


Figure 6. The S_{11} for the primary M-MSA design.

From the former Figure 6, it is clear that the simulated M-MSA doesn't cover a total band of the UWB systems. Whereas, the operating regions are only below the horizontal blue line. So, to overcome this problem the parameters and shape corrections process is applied.

5.2 Results for Optimised M-MSA Design

In this subsection, we will present the results for the M-MSA design after the parameters and shape modifications process.

a) M-MSA S_{11}

Figure 7 illustrates the archived S_{11} results for the simulated M-MSA after modification the dimensions and shape.

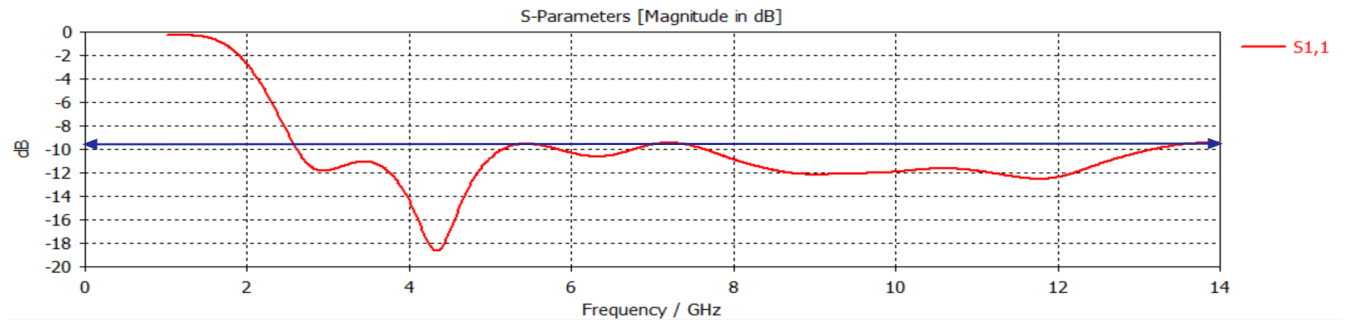


Figure 7. The S_{11} results for the simulated M-MSA after optimisation.

As presented in the recent Figure 7 the antenna covered the completed band of the UWB. This is due to applying the optimisation process on the dimensions and the shape of our M-MSA design.

b) M-MSA Gain

Under typical conditions, M-MSA exhibits a low gain due to the influence of substrate characteristics such as height and dielectric constant. Specifically, the gain improves when the height (h) is increased, but worsens when the

dielectric constant is increased. Since the primary design before the optimization process isn't covering the completed UWB frequency so there isn't a need to measure its gain. Figure 8 presents the M-MSA gain after the optimisation procedure.

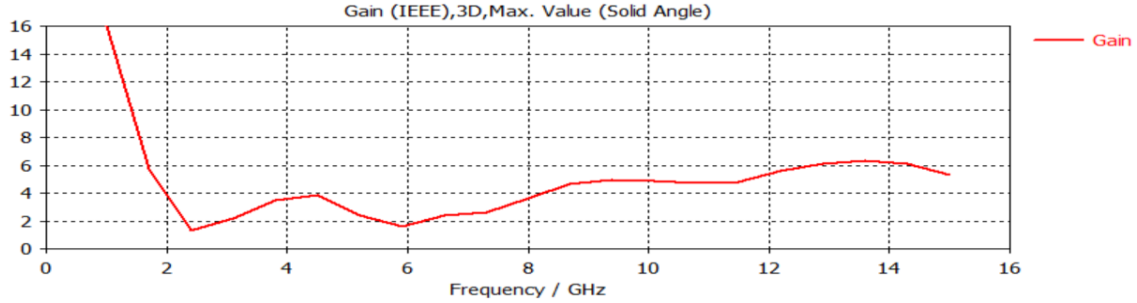


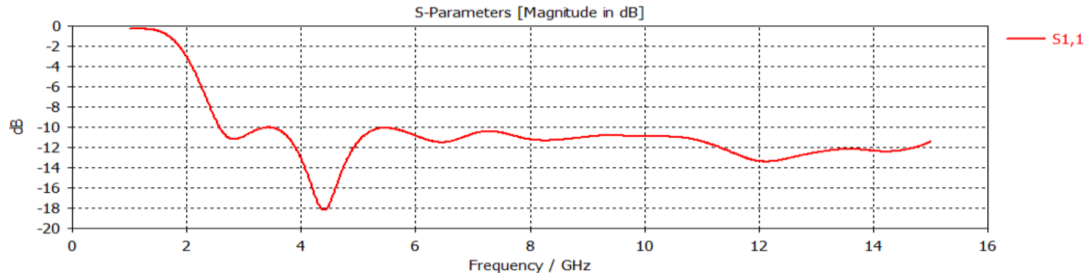
Figure 8. Total band gain for the proposed antenna after the modification process.

5.3 Results for M-MSA Design with Graphene

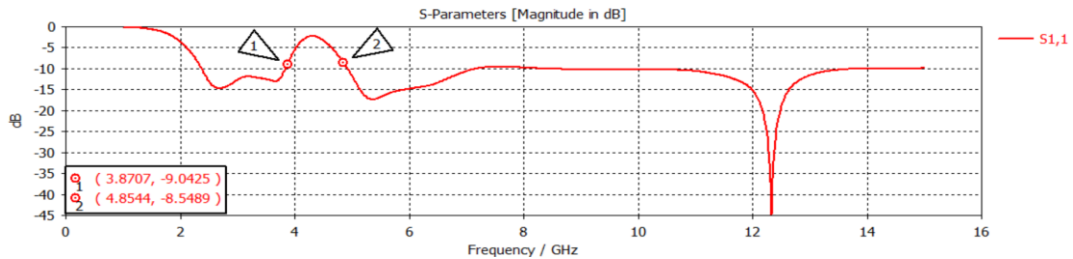
In this subsection, we will present the results for the M-MSA design after the engraving a small U-shaped aperture at the patch of the M-MSA.

a) M-MSA S_{11}

Figure 9 illustrates the archived S_{11} results for the simulated M-MSA after modification by adding the U-shaped aperture with graphene material at both ON/OFF cases.



(a) Graphene at ON case



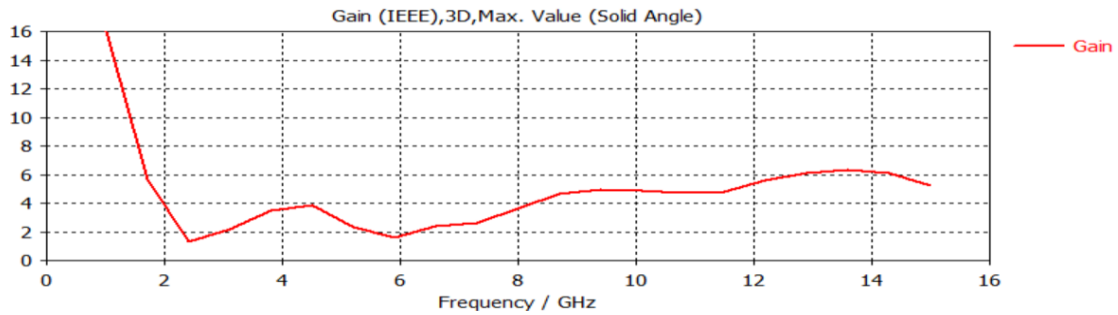
(b) Graphene at OFF case

Figure 9. The S_{11} for the M-MSA with U-shaped aperture and graphene.

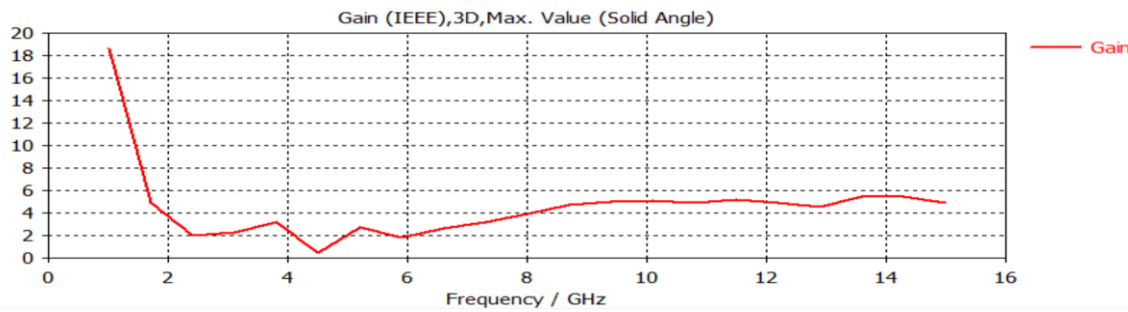
According on the reached results that exhibited in Figure 9 above, the graphene U-shaped apertures is acts as a controllable switch in the ON case the simulated M-MSA is working at the whole band of the UWB system and in the OFF case the effect of the aperture is appeared and created a bandgap in the UWB system aimed to reduce the interference in the range of 3.87-4.85 GHz.

b) M-MSA Gain

Figure 10 illustrates the archived gain results for the simulated M-MSA after modification by adding the U-shaped aperture with graphene material at both ON/OFF cases.



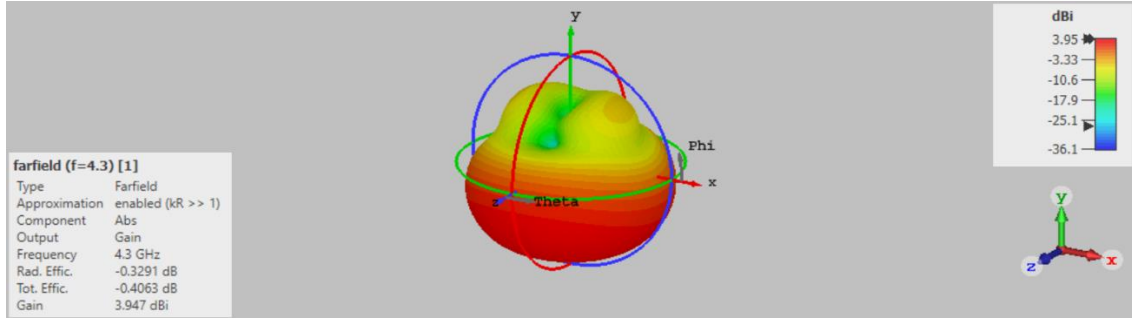
(a) Graphene at ON case



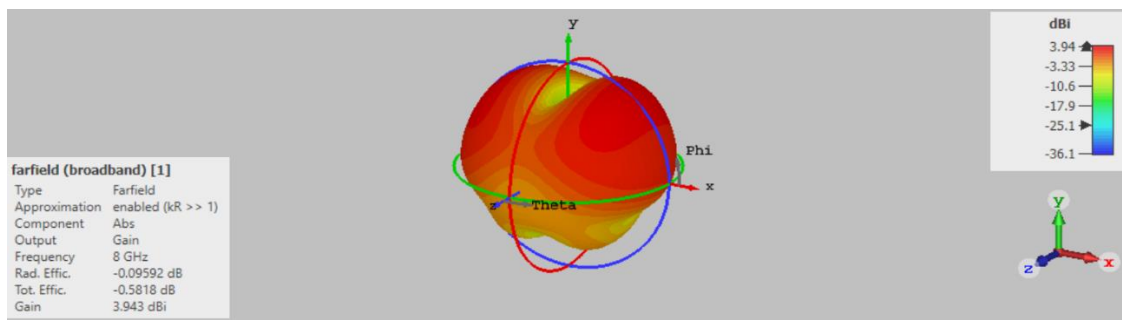
(b) Graphene at OFF case

Figure 10. The gain for the M-MSA with U-shaped aperture and graphene.

As exhibited in Figure 10, the obtained gain results at the OFF case in decreased to be around the zero at the bandgap region; this demonstrates that the simulated M-MSA will doesn't operate correctly due to the poor gain and operated in the rest of the band due to there isn't effect for the U-aperture at the rest of the band. In order to study the performance for the simulated M-MSA at the ON and OFF cases a gain monitor is created from the CST software at $f_r=4.3$ GHz which is the centre of the bandgap, as exhibited in Figure 11.



(a) Gain at ON case, $f_r = 4.3$ GHz



(b) Gain at OFF case, $f_r = 4.3$ GHz

Figure 11. The 3D gain results at $f_r = 4.3$ GHz.

6. CONCLUSION

M-MSA antennas are ideal for portable device integration due to their easy manufacture, low cost, and small size. UWB technology, used in many wireless applications, uses these antennas. UWB technology is used in low-power wireless applications such as wireless music, personal localization, indoor networks, radar, and high-resolution video transmission. Its frequency spectrum is 3.1 to 10.6 GHz. Due to its wide bandwidth, this frequency range is prone to interference. This paper develops, simulates, and optimises a modified compact square M-MSA that meets UWB standards to overcome this issue. The simulated M-MSA configuration has a substrate, partial ground plane, and square radiating patch printed on the same surface. The feeding technique uses a coplanar waveguide. To comply with the UWB range, M-MSA adjustments were made. In particular, the square patch corners at both lower borders adjacent to the feeding side were chopped. In conclusion, a U-shaped aperture in the radiating patch created a bandgap in the UWB system, minimising interference. The implanted aperture was filled with graphene to tune this bandgap. The bandgap can be eliminated by DC biasing graphene. In the absence of biasing, graphene has high impedance, preventing aperture current flow. The bandgap effect becomes evident at 3.87-4.85 GHz. The simulated M-MSA gained 1.288 to 6.284 dBi in the operational region (2.5-15 GHz).

REFERENCES

- Ahmad, S., Khan, S., Manzoor, B., Soruri, M., Alibakhshikenari, M., Dalarsson, M., & Falcone, F. (2022). A compact CPW-fed ultra-wideband multi-input-multi-output (MIMO) antenna for wireless communication networks. *IEEE Access*, 10, 25278-25289.
- Zhao, R., Li, H., Zhu, W., Wei, B., Zheng, C., & Lin, Q. (2023, July). A review of UWB positioning technology applications in personnel security management. In *Third International Conference on Digital Signal and Computer Communications (DSCC 2023)* (Vol. 12716, pp. 265-274). SPIE.
- Bastida Castillo, C. D. Gómez Carmona, E. De la Cruz Sánchez, and J. Pino Ortega, "Accuracy, intra-and inter-unit reliability, and comparison between GPS and UWB-based position-tracking systems used for time-motion analyses in soccer," in *European Journal of Sport Science*, vol. 18, no. 4, pp. 450-457, 2018.
- Chen, Y. Y., Huang, S. P., Wu, T. W., Tsai, W. T., Liou, C. Y., & Mao, S. G. (2020). UWB system for indoor positioning and tracking with arbitrary target orientation, optimal anchor location, and adaptive NLOS mitigation. *IEEE Transactions on Vehicular Technology*, 69(9), 9304-9314.
- Martalò, M., Perri, S., Verdano, G., De Mola, F., Monica, F., & Ferrari, G. (2021). Improved UWB TDoA-based positioning using a single hotspot for industrial IoT applications. *IEEE Transactions on Industrial Informatics*, 18(6), 3915-3925.
- Ghosh, D., & Sahu, P. K. (2016, September). UWB in healthcare. In *2016 International conference on electromagnetics in advanced applications (ICEAA)* (pp. 679-682). IEEE.
- Perdana, M. Y., Hariyadi, T., & Wahyu, Y. (2017, March). Design of vivaldi microstrip antenna for ultra-wideband radar applications. In *IOP Conference Series: Materials Science and Engineering* (Vol. 180, No. 1, p. 012058). IOP Publishing.
- Raval, B. T., Pimpalgaonkar, P. R., Chaurasia, M. R., & Upadhyaya, T. (2016). Review of ultra-wideband and design studies of patch antenna for ultra-wideband communication. In *1st International Conference on Automation in Industries (ICAI)* (pp. 100-105).
- Mahmood, S. N., Ishak, A. J., Ismail, A., Soh, A. C., Zakaria, Z., & Alani, S. (2020). ON-OFF body ultra-wideband (UWB) antenna for wireless body area networks (WBAN): a review. *IEEE Access*, 8, 150844-150863.
- Tiwari, P., & Malik, P. K. (2020, January). Design of UWB antenna for the 5G mobile communication applications: a review. In *2020 International conference on computation, automation and knowledge management (ICCAKM)* (pp. 24-30). IEEE.
- Werfelli, H., Tayari, K., Chaoui, M., Lahiani, M., & Ghariani, H. (2016, March). Design of rectangular microstrip patch antenna. In *2016 2nd International Conference on Advanced Technologies for Signal and Image Processing (ATSIP)* (pp. 798-803). IEEE.

- Hossain, I., Ahmed, T., & Kabir, H. (2022). Design of Rectangular Microstrip Patch Antenna at 3.3 GHz Frequency for S-band Applications. *Int. J. Eng., Manuf*, 12(4), 46-52.
- Abdulnabi, H. A., Shurij, M. A., & Sohrab, A. A. (2023). A Modified Polygon Shaped Microstrip Patch Antenna Array for Ultra-Wideband Applications. *Control Systems and Optimization Letters*, 1(2), 99-103.
- Alvarez, C. N., Cheung, R., & Thompson, J. S. (2017). Performance analysis of hybrid metal–graphene frequency reconfigurable antennas in the microwave regime. *IEEE Transactions on Antennas and Propagation*, 65(4), 1558-1569.